

Transmission Line Model for Charge and Spin Transport in Channels with Spin-Momentum Locking

Shehrin Sayed* and Supriyo Datta†

School of Electrical and Computer Engineering, Purdue University, West Lafayette, IN 47907, USA

Seokmin Hong

Center for Spintronics, Korea Institute of Science and Technology, Seoul 02792, Republic of Korea.

We provide a transmission line representation for channels exhibiting spin-momentum locking (SML) which can be used for both time-dependent and steady-state 1D transport analysis on a wide variety of materials with spin-orbit coupling such as topological insulators, heavy metals, and narrow bandgap semiconductors. This model is based on the time-dependent semiclassical equations obtained from the Boltzmann formalism under linear response approximation using four electrochemical potentials for four groups of electronic states (U^+ , D^+ , U^- , and D^-) depending on the spin index (U , D) and the sign of the x -component of the group velocity ($+$, $-$). A key parameter in this formalism is the degree of SML described by $p_0 = (M - N) / (M + N)$, M and N being number of modes for (U^+ , D^-) and (U^- , D^+) groups respectively. For normal metal channels ($p_0 = 0$), the model decouples into the well known transmission line model for charge and the time-dependent version of Valet-Fert equation respectively. Our model shows that the charge and spin signals travel with two distinct velocities resulting in well-known spin-charge separation which is expected to persist even in the presence of SML i.e. $p_0 \neq 0$. Similar arguments have been discussed previously although there exists counter argument that the spin-orbit coupling may destroy the spin-charge separation. However, our model predicts that the lower velocity signal is purely spin while the higher velocity signal is largely charge with an additional spin component proportional to p_0 , which has not been noted before.

I. INTRODUCTION

Background: Transport properties in materials with spin-orbit coupling (SOC) are of great interest for potential spintronic applications, especially because of unique spin-momentum locking (SML) observed in diverse classes of materials such as topological insulator (TI) [1–3], heavy metals [4–9], and narrow bandgap semiconductors [10–12]. There has been an immense effort to model the interplay between spin and charge in such materials using time-dependent classical [13] or quantum Boltzmann equation [14, 15], nonequilibrium Green’s function [16–20], phenomenological equations coupled to magnet dynamics [21], and time-independent diffusion equation used to explain bulk spin Hall effect [22].

Previously, we proposed a time-independent semiclassical model for such materials exhibiting SML [23, 24], obtained from the Boltzmann formalism using four electrochemical potentials for four groups of electronic states (U^+ , D^+ , U^- , and D^-) depending on the spin index (U , D) and the sign of the x -component of the group velocity ($+$, $-$). This classification can be viewed as a combination of the two well-known approaches for normal metals: (i) Valet-Fert equation with two electrochemical potentials for U and D states [25] and (ii) mesoscopic view with

two electrochemical potentials for $+$ and $-$ states [26]. In our generalized view, U^+ (and U^-) states have same number of modes M (and N) as D^- (and D^+) states due to time reversal symmetry. The degree of SML is given by [23, 24]

$$p_0 = \frac{M - N}{M + N}, \quad (1)$$

where M and N are evaluated at Fermi energy for zero temperature and in general require thermal averaging. For normal metal (NM) channels $p_0 = 0$ i.e. $M = N$.

For a perfect topological insulator (TI) $p_0 = 1$ i.e. $N = 0$, however, gets effectively lowered by the presence of parallel channels. p_0 has been quantified for different TIs by a number of groups [27–33] by measuring the charge current induced spin voltage using a ferromagnetic (FM) contact, motivated by a theoretical proposal [20]. For a Rashba channel with a coupling coefficient α_R , $p_0 \approx \alpha_R k_F / (2E_F) \ll 1$ [12, 20] which can be quantified with similar spin voltage measurements [10, 11]. k_F and E_F are the Fermi wave vector and Fermi energy respectively. Recently, spin voltage measurements have been reported on heavy metals like platinum [34, 35] and gold [36]. Moreover, our semiclassical model predicted a unique three resistance state on SML channel with two FM contacts in a multi-terminal spin valve structure [23], which was recently observed on a heavy metal [34, 35]. These experiments can be quantified by p_0 , however, the underlying mechanism is subject to active debate [37–39] and could involve a bulk spin Hall effect [7, 22, 40] or

* ssayed@purdue.edu

† datta@purdue.edu

interface Rashba-like channel [8, 41–43].

This Work: In this paper, we extend our prior semi-classical equations [23] to include time-dependence and translate it to a transmission line model with two component (charge and z -component of spin) voltages and currents. The model can be used for both time-dependent and steady-state 1D transport analysis on multi-contact based structures implemented with materials exhibiting SML. This model is a new addition to our multi-physics spin-circuit framework [44] which has been previously used to explain experiments and evaluate spin-based device proposals [45, 46].

For NM channels (i.e. $p_0 = 0$), the model decouples into well-known transmission line model for charge [47–49] and time-dependent version of Valet-Fert equation [25] respectively. The model suggests that depending on the channel cross-section, the charge signal can travel faster than the spin signal resulting in well-known spin-charge separation [47, 50–52], which we argue is true even for channels with SML i.e. $p_0 \neq 0$. Spin-charge separation has been discussed in the past considering the presence of spin-orbit coupling (SOC) [53–55] although there exists counter arguments that the presence of SOC destroys the spin-charge separation [56]. However, we predict that the charge signal in SML channels accompanies an additional spin component proportional to p_0 having the same velocity as the charge, which has not been discussed before.

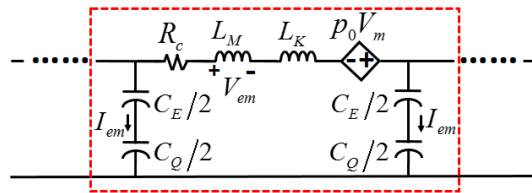
Note that the proposed model does not take into account effects such as spin precession, which involves off-diagonal elements of the density matrix which we assume to be negligible. An extension of this model to include x and y components of spin could possibly address such issues, as done earlier for materials without SOC (see [45], and references therein).

Outline: The paper is organized as follows. In Section II, we describe the transmission line model and discuss the spin-charge separation in terms of spin and charge signal velocities. We show that in channels with SML there exists an additional spin component accompanied by the charge signal. In Section III, we derive the transmission line model starting from the 1D Boltzmann transport equation with four electrochemical potentials and extract the model parameters in terms of microscopic quantities. We discuss different scattering mechanisms in the channels and their effects on charge and spin transport. In Section IV, we incorporate external contact which can be either normal metal or ferromagnet and discuss different effects on channel. Finally, in Section V we end with a brief summary.

II. TRANSMISSION LINE MODEL

Charge and Spin Models: The model has two components: charge and z -component of spin with coupling

(a) Charge transmission line



(b) Spin transmission line

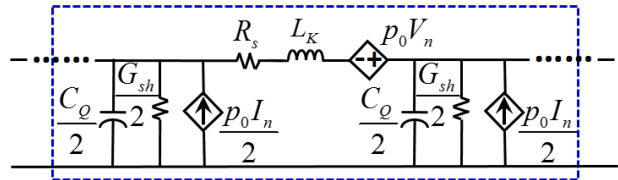


FIG. 1. Transmission line model for channels with spin-momentum locking (SML). The model has two components: (a) charge (corresponds to Eq. (2)) and (b) spin (corresponds to Eq. (3)), with coupling between them described by degree of SML p_0 (see Eq. (1)). Coupling between charge and spin are modeled by dependent voltage and current sources with $V_m = \eta_c V_s$, $V_n = \eta_s V_c + r_m I_{em}$, and $I_n = \gamma_s I_c - g_m V_{em}$.

between them characterized by p_0 . The charge equations (also see Fig. 1(a)) are given by

$$\left(\frac{1}{C_E} + \frac{1}{C_Q} \right)^{-1} \frac{\partial}{\partial t} V_c = -\frac{\partial}{\partial x} I_c, \quad (2)$$

$$(L_K + L_M) \frac{\partial}{\partial t} I_c + R_c I_c = -\frac{\partial}{\partial x} V_c + p_0 \eta_c V_s,$$

and the spin equations (also see Fig. 1(b)) are given by

$$C_Q \frac{\partial}{\partial t} V_s + G_{sh} V_s + p_0 g_m V_{em} = -\frac{\partial}{\partial x} I_s + p_0 \gamma_s I_c, \quad (3)$$

$$L_K \frac{\partial}{\partial t} I_s + R_s I_s - p_0 r_m I_{em} = -\frac{\partial}{\partial x} V_s + p_0 \eta_s V_c,$$

where C_E and C_Q are the electrostatic and quantum capacitances per unit length, L_M and L_K are the magnetic and kinetic inductances per unit length, R_c and R_s are the charge and spin resistances per unit length, and G_{sh} is the shunt spin conductance per unit length which captures the spin lost in the channel due to the spin relaxation. I_{em} is the current flowing through the electrostatic capacitor and V_{em} is the voltage across the magnetic inductor. r_m and g_m are transient charge-spin coupling coefficient which are in the units of resistance and conductance per unit length respectively and depend on the scattering processes in the channel. Here, I_c , I_s and V_c , V_s are charge and spin currents and voltages along \hat{x} -direction. Spin polarization is in the \hat{z} -direction and \hat{y} -direction is out-of-plane. Detailed derivation of Eqs. (2) and (3) will be discussed in the next section where the model parameters will be extracted in terms of microscopic quantities in the channel.

For NM channels ($p_0 = 0$), the charge model in Eq. (2) reduces to the well-known transmission line model for charge transport in quantum wires, first derived from Luttinger liquid theory [47, 48] and then from Boltzmann transport equation with one electrochemical potential [49]. For $p_0 = 0$, the spin model in Eq. (3) can be considered as time-dependent form of Valet-Fert equation [25]. Similar spin model was previously proposed based on Luttinger liquid theory [47] which did not take into account the spin relaxation processes in the channel. We consider spin relaxation process by shunt spin conductance G_{sh} which comes straight from 1D Boltzmann formalism with four electrochemical potentials.

Charge and Spin Velocity: The velocities for charge and spin signals can be derived by finding the eigenvalues of Eqs. (2) and (3) assuming low loss limit. In addition, we find the corresponding eigenvectors as well to analyze the coupling between spin and charge in the channel due to SML. See Appendix A for the detailed derivation.

The lower velocity eigenvalue is given by

$$v_{g,s} = \pm \frac{1}{\sqrt{L_K C_Q}} = \pm \langle v_x \rangle, \quad (4)$$

which is determined by quantum capacitance C_Q and kinetic inductance L_K , resulting in thermally averaged electron velocity $\langle v_x \rangle$. The corresponding eigenvector is given by

$$\begin{Bmatrix} V_c \\ I_c \end{Bmatrix} = \begin{Bmatrix} 0 \\ 0 \end{Bmatrix}, \text{ and } \begin{Bmatrix} V_s \\ I_s \end{Bmatrix} = \begin{Bmatrix} \pm \sqrt{\frac{L_K}{C_Q}} \\ 1 \end{Bmatrix}, \quad (5)$$

which shows that the lower velocity signal is purely spin and no charge accompanies the signal even in channels with SML i.e. $p_0 \neq 0$.

The higher velocity eigenvalue is given by

$$v_{g,c} = \pm \frac{1}{\sqrt{L_{eff} C_{eff}}}, \quad (6)$$

where C_{eff} is a series combination of C_E and C_Q and L_{eff} is a series combination of L_M and L_K . The corresponding eigenvector is given by

$$\begin{Bmatrix} V_c \\ I_c \end{Bmatrix} = \begin{Bmatrix} \pm \sqrt{\frac{L_{eff}}{C_{eff}}} \\ 1 \end{Bmatrix}, \text{ and } \begin{Bmatrix} V_s \\ I_s \end{Bmatrix} = \frac{p_0}{v_{g,c}^2 - v_{g,s}^2} \begin{Bmatrix} -g_m \frac{L_M}{C_Q} v_{g,c}^2 + r_m v_{g,s}^2 \\ \pm \frac{v_{g,c} v_{g,s}}{L_K} \left(-g_m \frac{L_M}{C_Q} + r_m \right) \end{Bmatrix}, \quad (7)$$

which shows that the higher velocity signal is largely charge which will be accompanying an additional spin signal proportional to p_0 which has not been discussed before. This additional spin component vanishes in a

NM channel where there is no SML (i.e. $p_0 = 0$) and the signal is purely charge. Further evaluation of this high velocity spin component we leave as future work.

The quantum capacitance C_Q is proportional to the total number of modes ($M + N$) in the channel while the kinetic inductance L_K is inversely proportional to $M + N$. $M + N$ is proportional to the channel width (for 2D) or cross-sectional area (for 3D) [57]. For a conductor with very large cross-section, we have $C_E \ll C_Q$ and $L_M \gg L_K$ which makes the velocity in Eq. (6) equal to the speed of light $c = 1/\sqrt{L_M C_E}$. On the contrary, for a conductor with very small cross-section like quantum wires, we have $C_E \gg C_Q$ and $L_M \ll L_K$ yielding velocity in Eq. (6) equal to the thermally averaged electron velocity $\langle v_x \rangle = 1/\sqrt{L_K C_Q}$, same as Eq. (4). Thus depending on the channel cross-section, the charge signal can propagate at a velocity in the range: $\langle v_x \rangle \leq v_{g,c} \leq c$, which has been discussed earlier in the context of transport in quantum wires with no SML ($p_0 = 0$) [47, 49].

Spin-Charge Separation: Eqs. (4) and (6) suggest that depending on the cross-section of the channel, the spin signal travels slower than the charge signal ($v_{g,s} \leq v_{g,c}$) resulting in spin-charge separation, which is well-established for channels without SML (i.e. $p_0 = 0$) from Luttinger liquid theory (see for example, Refs. [47, 50–52], and references therein). Note that the arguments from Eqs. (4) and (6) are independent of p_0 (see Appendix A) and spin-charge separation persists even in channels with SML (i.e. $p_0 \neq 0$). Similar arguments have been discussed previously by considering spin-orbit coupling (SOC) [53–55] although there exists argument that the presence of SOC may destroy the spin-charge separation [56]. We argue from Eqs. (4)-(7) that these two distinct velocities persist ($v_{g,c}$ and $v_{g,s}$) even in the channels with SOC exhibiting SML (i.e. $p_0 \neq 0$), however, in SML channels an additional spin signal proportional to p_0 accompanies the charge signal at the same velocity as the charge ($v_{g,c}$).

III. SEMICLASSICAL FORMALISM

Boltzmann Transport Equation: In this section, we derive the transmission line model in Eqs. (2) and (3) assuming a structure where the spatial variations and the applied fields are along \hat{x} -direction. We start from the time-dependent Boltzmann transport equation, given by

$$\frac{\partial f}{\partial t} + v_x \frac{\partial f}{\partial x} + F_x \frac{\partial f}{\partial p_x} = \sum_{\vec{p}', s'} S(\vec{p}, s \leftrightarrow \vec{p}', s') (f - f'), \quad (8)$$

where $f \equiv f(x, t, \vec{p}, s)$ is the occupation factor of a state for a particular position x , time t , momentum \vec{p} and spin index $s = \pm 1$, $f' \equiv f(x, t, \vec{p}', s')$ with momentum \vec{p}' and spin index $s' = \pm 1$, $v_x = \partial E / \partial p_x$ is the x -component of the group velocity, $F_x = -\partial E / \partial x$ is the force on electrons

along \hat{x} -direction, and E is the total energy. Note that the spin index $+1$ and -1 correspond to up (U) and down (D) spin polarized states for a particular \vec{p} . We have assumed elastic scattering so that the scattering rates are same in both directions $S(\vec{p}, s \rightarrow \vec{p}', s') = S(\vec{p}', s' \rightarrow \vec{p}, s) \equiv S(\vec{p}, s \leftrightarrow \vec{p}', s')$.

We write the occupation factor f in terms of an electrochemical potential $\mu \equiv \mu(x, t, \vec{p}, s)$, in the form

$$f(x, t, \vec{p}, s) = \frac{1}{1 + \exp\left(\frac{E(x, t, \vec{p}, s) - \mu(x, t, \vec{p}, s)}{k_B T}\right)}, \quad (9)$$

where k_B is the Boltzmann constant, T is the temperature.

Linear Response: We apply a variable transform $\xi = E - \mu$ on the left hand side of Eq. (8). On the right hand side of Eq. (8), we expand both f and f' into Taylor series around

$$f_0 = \frac{1}{1 + \exp\left(\frac{(E(x, \vec{p}, s) - \mu_0)}{k_B T}\right)}, \quad (10)$$

with constant electrochemical potential μ_0 and apply linear response approximation. Thus Eq. (8) can be written as (see Appendix B for details of the derivation)

$$\begin{aligned} & \left(-\frac{\partial f_0}{\partial E}\right) \left(\frac{\partial \mu}{\partial t} - \frac{\partial E}{\partial t} + v_x \frac{\partial \mu}{\partial x} + F_x \frac{\partial \mu}{\partial p_x}\right) \\ &= -\sum_{\vec{p}', s'} S(\vec{p}, s \leftrightarrow \vec{p}', s') \left(-\frac{\partial f_0}{\partial E}\right) (\mu - \mu'). \end{aligned} \quad (11)$$

We neglect the term $F_x(\partial\mu/\partial p_x)$ under the linear response approximation [57] as

$$\begin{aligned} & \left(-\frac{\partial f_0}{\partial E}\right) \left(\frac{\partial \mu}{\partial t} - \frac{\partial E}{\partial t} + v_x \frac{\partial \mu}{\partial x}\right) \\ &= -\sum_{\vec{p}', s'} S(\vec{p}, s \leftrightarrow \vec{p}', s') \left(-\frac{\partial f_0}{\partial E}\right) (\mu - \mu'). \end{aligned} \quad (12)$$

Dispersion Relation: We start from the following Rashba Hamiltonian

$$\mathcal{H} = \frac{|\vec{p} - q\vec{A}|^2}{2m} I_{2 \times 2} - v_0 \left(\vec{\sigma} \times (\vec{p} - q\vec{A})\right) \cdot \hat{y} + U_E I_{2 \times 2}. \quad (13)$$

Here, $I_{2 \times 2}$ is a 2×2 identity matrix, \vec{p} and \vec{A} are the momentum and vector magnetic potential respectively in the z - x plane, $\vec{\sigma}$ is the Pauli's matrices, v_0 is the Rashba coefficient, U_E is the electrostatic potential, m is the electron mass, and q is the electron charge. Eigenstates of Eq. (13) are given by

$$E(\vec{p}, s) = \frac{|\vec{p} - q\vec{A}|^2}{2m} + s v_0 |\vec{p} - q\vec{A}| + U_E,$$

with \vec{p} is confined to the z - x plane. We assume that U_E and \vec{A} varies slowly with x and t , so that in the semiclassical approximation we have

$$E(x, t, \vec{p}, s) = \frac{|\vec{p} - q\vec{A}(x, t)|^2}{2m} + s v_0 |\vec{p} - q\vec{A}(x, t)| + U_E(x, t). \quad (14)$$

Differentiating Eq. (14) with respect to t yields

$$\frac{\partial E}{\partial t} = \vec{v} \cdot \left(-q \frac{\partial \vec{A}}{\partial t}\right) + \frac{\partial U_E}{\partial t}, \quad (15)$$

where $\vec{v} = \nabla_{\vec{p}} E$ (see Appendix C for the derivation).

Electromagnetics: The electrostatic potential U_E is related to the total charge Q by the electrostatic capacitance C_E as $U_E/q = Q/C_E$. The vector magnetic potential \vec{A} is related to the charge current in the channel by the magnetic inductance L_M . We assume $\vec{A} \equiv \hat{x} A_x = \hat{x} L_M I_c$ where I_c is the charge current along \hat{x} -direction. Thus Eq. (15) can be written as

$$\frac{\partial E}{\partial t} = -q v_x L_M \frac{\partial I_c}{\partial t} + \frac{q}{C_E} \frac{\partial Q}{\partial t}. \quad (16)$$

We combine Eq. (12) with Eq. (16) to get

$$\begin{aligned} & \left(\frac{\partial f_0}{\partial E}\right) \left(\frac{\partial \mu}{\partial t} + v_x \frac{\partial \mu}{\partial x} + q v_x L_M \frac{\partial I_c}{\partial t} - \frac{q}{C_E} \frac{\partial Q}{\partial t}\right) \\ &= -\sum_{\vec{p}', s'} S(\vec{p}, s \leftrightarrow \vec{p}', s') \left(\frac{\partial f_0}{\partial E}\right) (\mu - \mu'). \end{aligned} \quad (17)$$

Classification: We classify all \vec{p}, s states into four groups based on the sign of v_x (+ or -) and the spin index $s = \pm 1$, given by

$$\mathfrak{R} : \begin{cases} U^+ \in \{\vec{p}, s \mid v_x > 0, s = +1\}, \\ D^- \in \{\vec{p}, s \mid v_x < 0, s = -1\}, \\ U^- \in \{\vec{p}, s \mid v_x < 0, s = +1\}, \text{ and} \\ D^+ \in \{\vec{p}, s \mid v_x > 0, s = -1\}. \end{cases} \quad (18)$$

where $s = +1$ and -1 denote up (U) and down (D) spins with respect to the spin quantization axis defined by $\hat{y} \times (\vec{p} - q\vec{A})$, which is different for each direction of \vec{p} . Such classification can be mapped onto the two Fermi circles of a Rashba channel (see Fig. 2(a)). The large circle corresponds to U^+ and D^- groups which share the same number of modes $n_m(U^+) = n_m(D^-) = M$ satisfying the time-reversal symmetry. Similarly, the small circle corresponds to U^- and D^+ groups sharing the same number of modes $n_m(U^-) = n_m(D^+) = N$. Note that the eigenstates belonging to each of the four half Fermi circles in Fig. 2(a) has an average spin polarization along \hat{z} -direction with an averaging factor of $\alpha = 2/\pi$, which we will use later when writing spin currents and voltages.

Averaging: We define the thermal average of a variable $\psi \equiv \psi(\vec{p}, s)$ within each of the group $\vec{p}, s \in \mathfrak{R}$ as

$$\langle \psi \rangle_{\vec{p}, s \in \mathfrak{R}} = \frac{\sum_{\vec{p}, s \in \mathfrak{R}} \left(-\frac{\partial f_0}{\partial E} \right) \psi(\vec{p}, s)}{\sum_{\vec{p}, s \in \mathfrak{R}} \left(-\frac{\partial f_0}{\partial E} \right)}. \quad (19)$$

We sum both sides of Eq. (17) over all \vec{p} states within range $\vec{p}, s \in \mathfrak{R}$ in the z - x plane as

$$\begin{aligned} & \frac{D_0(\mathfrak{R})}{2} \frac{\partial \langle \mu \rangle}{\partial t} + \frac{D_0(\mathfrak{R})}{2} \frac{\partial \langle v_x \mu \rangle}{\partial x} \\ & + \frac{q D_0(\mathfrak{R})}{2} \langle v_x \rangle L_M \frac{\partial I_c}{\partial t} - \frac{q}{C_E} \frac{D_0(\mathfrak{R})}{2} \frac{\partial Q}{\partial t} \\ & = - \sum_{\vec{p}, s \in \mathfrak{R}} \sum_{\vec{p}', s'} S(\vec{p}, s \leftrightarrow \vec{p}', s') \left(-\frac{\partial f_0}{\partial E} \right) (\mu - \mu'). \end{aligned} \quad (20)$$

Here, $D_0(\mathfrak{R})$ is the thermally averaged density of states within $\vec{p}, s \in \mathfrak{R}$ given by

$$\frac{D_0(\mathfrak{R})}{2} = \sum_{\vec{p}, s \in \mathfrak{R}} \left(-\frac{\partial f_0}{\partial E} \right), \quad (21)$$

where the factor of 2 appeared since we are summing over all s states. Note that $D_0(U^+) = D_0(D^-)$ and $D_0(U^-) = D_0(D^+)$ due to time-reversal symmetry.

We make the following assumption in Eq. (20)

$$\langle v_x \mu \rangle \approx \langle v_x \rangle \langle \mu \rangle,$$

which yields

$$\begin{aligned} & \frac{D_0(\mathfrak{R})}{2} \frac{\partial \langle \mu \rangle}{\partial t} + \frac{D_0(\mathfrak{R})}{2} \langle v_x \rangle \frac{\partial \langle \mu \rangle}{\partial x} \\ & + \frac{q D_0(\mathfrak{R})}{2} \langle v_x \rangle L_M \frac{\partial I_c}{\partial t} - \frac{q}{C_E} \frac{D_0(\mathfrak{R})}{2} \frac{\partial Q}{\partial t} \\ & = - \sum_{\vec{p}, s \in \mathfrak{R}} \sum_{\vec{p}', s'} S(\vec{p}, s \leftrightarrow \vec{p}', s') \left(-\frac{\partial f_0}{\partial E} \right) (\mu - \mu') + \frac{i_{ext}}{q}. \end{aligned} \quad (22)$$

Note that the term i_{ext}/q on the right hand side has been added to take into account the total current entering into $\vec{p}, s \in \mathfrak{R}$ states of the channel an external contact.

The number of modes within $\vec{p}, s \in \mathfrak{R}$ in the channel is given by [57]

$$n_m(\mathfrak{R}) = \frac{\hbar D_0 | \langle v_x \rangle |}{2L}, \quad (23)$$

where $| \langle v_x \rangle |$ is the magnitude of $\langle v_x \rangle$ and L is the channel length. Note that $| \langle v_x \rangle |$ is same in all four groups for the Rashba Hamiltonian considered here (see Appendix C).

Thus Eq. (22) can be written as

$$\begin{aligned} & \frac{n_m(\mathfrak{R})}{| \langle v_x \rangle |} \frac{\partial \langle \mu \rangle}{\partial t} + \text{sgn}(\langle v_x \rangle) n_m(\mathfrak{R}) \frac{\partial \langle \mu \rangle}{\partial x} \\ & + \text{sgn}(\langle v_x \rangle) q n_m(\mathfrak{R}) L_M \frac{\partial I_c}{\partial t} - \frac{q}{C_E} \frac{n_m(\mathfrak{R})}{| \langle v_x \rangle |} \frac{\partial Q}{\partial t} \\ & = - \frac{\hbar}{L} \sum_{\vec{p}, s \in \mathfrak{R}} \sum_{\vec{p}', s'} S(\vec{p}, s \leftrightarrow \vec{p}', s') \left(-\frac{\partial f_0}{\partial E} \right) (\mu - \mu') + \frac{\hbar i_{ext}}{q L}, \end{aligned} \quad (24)$$

Eq. (24) applies to each group in Eq. (18) with an average electrochemical potential given by $\langle \mu \rangle_{\vec{p}, s \in U^+} \equiv \mu(U^+)$, $\langle \mu \rangle_{\vec{p}, s \in D^-} \equiv \mu(D^-)$, $\langle \mu \rangle_{\vec{p}, s \in U^-} \equiv \mu(U^-)$, and $\langle \mu \rangle_{\vec{p}, s \in D^+} \equiv \mu(D^+)$ respectively.

Scattering Matrix: We make the following assumption

$$\langle S \mu \rangle \approx \langle S \rangle \langle \mu \rangle,$$

which when applied to the term related to scattering rate on the right hand side of Eq. (24) becomes a matrix under such classification (see Appendix D for details), given by

$$[S] = \begin{bmatrix} -u_1 & \hat{S}_{U^+ \leftrightarrow D^-} & \hat{S}_{U^+ \leftrightarrow U^-} & \hat{S}_{U^+ \leftrightarrow D^+} \\ \hat{S}_{U^+ \leftrightarrow D^-} & -u'_1 & \hat{S}_{D^- \leftrightarrow U^-} & \hat{S}_{D^- \leftrightarrow D^+} \\ \hat{S}_{U^+ \leftrightarrow U^-} & \hat{S}_{D^- \leftrightarrow U^-} & -u_2 & \hat{S}_{U^- \leftrightarrow D^+} \\ \hat{S}_{U^+ \leftrightarrow D^+} & \hat{S}_{D^- \leftrightarrow D^+} & \hat{S}_{U^- \leftrightarrow D^+} & -u'_2 \end{bmatrix}, \quad (25)$$

where

$$\begin{aligned} u_1 &= \hat{S}_{U^+ \leftrightarrow D^-} + \hat{S}_{U^+ \leftrightarrow U^-} + \hat{S}_{U^+ \leftrightarrow D^+}, \\ u'_1 &= \hat{S}_{U^+ \leftrightarrow D^-} + \hat{S}_{D^- \leftrightarrow U^-} + \hat{S}_{D^- \leftrightarrow D^+}, \\ u_2 &= \hat{S}_{U^+ \leftrightarrow U^-} + \hat{S}_{D^- \leftrightarrow U^-} + \hat{S}_{U^- \leftrightarrow D^+}, \text{ and} \\ u'_2 &= \hat{S}_{U^+ \leftrightarrow D^+} + \hat{S}_{D^- \leftrightarrow D^+} + \hat{S}_{U^- \leftrightarrow D^+}. \end{aligned}$$

The scattering matrix is such that the sum of each column is zero satisfying the charge conservation and the sum of each row is zero satisfying the zero current requirement under equal potential. The scattering rates are given by

$$\hat{S}_{\mathfrak{R} \leftrightarrow \mathfrak{R}'} = \frac{\hbar}{L} \sum_{\vec{p}, s \in \mathfrak{R}} \sum_{\vec{p}', s' \in \mathfrak{R}'} \left(-\frac{\partial f_0}{\partial E} \right) S(\vec{p}, s \leftrightarrow \vec{p}', s'). \quad (26)$$

In addition, the time-reversal symmetry requires that

$$\hat{S}_{U^+ \leftrightarrow U^-} = \hat{S}_{D^- \leftrightarrow D^+} \text{ and } \hat{S}_{U^+ \leftrightarrow D^+} = \hat{S}_{D^- \leftrightarrow U^-}.$$

There are three types of scattering processes considered in the channel: (a) reflection with spin flip $r_{s1} = \hat{S}_{U^+ \leftrightarrow D^-}$ and $r_{s2} = \hat{S}_{U^- \leftrightarrow D^+}$, (b) reflection without spin flip $r = \hat{S}_{U^+ \leftrightarrow U^-} = \hat{S}_{D^- \leftrightarrow D^+}$, and (c) transmission with spin flip $t_s = \hat{S}_{U^+ \leftrightarrow D^+} = \hat{S}_{D^- \leftrightarrow U^-}$.

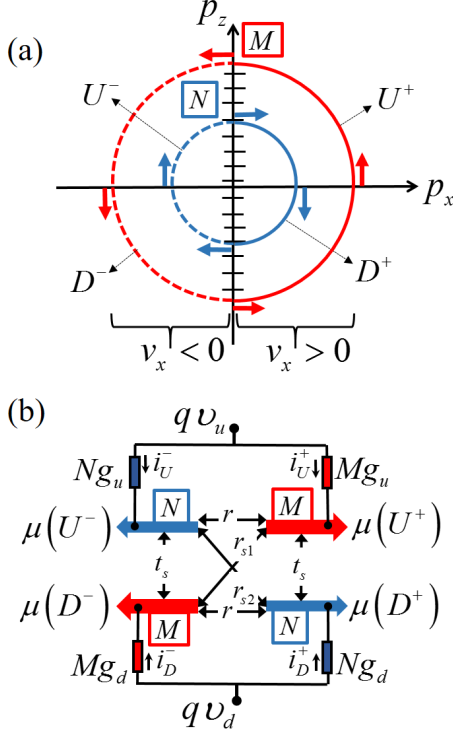


FIG. 2. (a) Two Fermi circles of a Rashba channel with spin-momentum locking having opposite spin polarizations at a given energy E_F . Left (right) half of each circle represents negative (positive) group velocity. The large circle corresponds to the large number of modes M in the channel and have a net spin polarization along $+\hat{z}$ ($-\hat{z}$) on right (left) side. The small circle corresponds to smaller number of modes N and have net spin polarization along $-\hat{z}$ ($+\hat{z}$) on right (left) side. We classify all electronics states into four groups based on the z -component of spin polarization (up (U), down (D)) and the sign of x -component of the group velocity ($+$, $-$). (b) Assuming high scattering among states in each individual groups, we assign four electrochemical potentials for these four groups: $\mu(U^+)$, $\mu(U^-)$, $\mu(D^+)$, and $\mu(D^-)$. External contact is modeled as up (v_u) and down (v_d) spin voltages applied to up and down states of the channel through up (g_u) and down (g_d) spin conductances per mode, respectively. Four different currents (i_U^+ , i_D^+ , i_U^- , and i_D^-) enter the four different groups in the channel. The contact can be either normal metal $g_u = g_d$ or ferromagnet $g_u \neq g_d$.

Semiclassical Equations: Eq. (24) for each group in

Eq. (18) is given as

$$\begin{aligned} & \frac{1}{|\langle v_x \rangle|} \frac{\partial}{\partial t} \begin{Bmatrix} M\tilde{\mu}(U^+) \\ M\tilde{\mu}(D^-) \\ N\tilde{\mu}(U^-) \\ N\tilde{\mu}(D^+) \end{Bmatrix} + \frac{\partial}{\partial x} \begin{Bmatrix} M\tilde{\mu}(U^+) \\ -M\tilde{\mu}(D^-) \\ -N\tilde{\mu}(U^-) \\ N\tilde{\mu}(D^+) \end{Bmatrix} \\ &= \begin{bmatrix} -u_1 & r_{s1} & r & t_s \\ r_{s1} & -u_1 & t_s & r \\ r & t_s & -u_2 & r_{s2} \\ t_s & r & r_{s2} & -u_2 \end{bmatrix} \begin{Bmatrix} \tilde{\mu}(U^+) \\ \tilde{\mu}(D^-) \\ \tilde{\mu}(U^-) \\ \tilde{\mu}(D^+) \end{Bmatrix} \\ &- qL_M \frac{\partial I_c}{\partial t} \begin{Bmatrix} M \\ -M \\ -N \\ N \end{Bmatrix} + \frac{q}{|\langle v_x \rangle|} \frac{\partial Q}{\partial t} \begin{Bmatrix} M \\ M \\ N \\ N \end{Bmatrix} + \frac{h}{q} \begin{Bmatrix} i_U^+ \\ i_D^- \\ i_U^- \\ i_D^+ \end{Bmatrix}. \end{aligned} \quad (27)$$

Note that the electrochemical potentials are referenced with respect to the constant μ_0 i.e. $\tilde{\mu} = \mu - \mu_0$. i_U^+ , i_D^- , i_U^- , and i_D^+ are the currents per unit length entering into the four groups from an external contact (see Fig. 2(b)), which will be discussed in the next section. In steady-state, Eq. (27) reduces to our prior model [23].

Charge-Spin Conversion: The charge and spin voltages and currents in the channel are defined in terms of the four average electrochemical potentials as [24]

$$\begin{Bmatrix} I_c R_B \\ 2V_s \\ 2V_c \\ I_s R_B \end{Bmatrix} = \frac{q}{h} R_B \begin{bmatrix} 1 & -1 & -1 & 1 \\ \alpha & -\alpha & \alpha & -\alpha \\ 1 & 1 & 1 & 1 \\ \alpha & \alpha & -\alpha & -\alpha \end{bmatrix} \begin{Bmatrix} M\tilde{\mu}(U^+) \\ M\tilde{\mu}(D^-) \\ N\tilde{\mu}(U^-) \\ N\tilde{\mu}(D^+) \end{Bmatrix}, \quad (28)$$

where $\alpha = 2/\pi$ is an angular averaging factor for average z -spins on a half Fermi circle (see Fig. 2(a)) [20, 23, 24] and $R_B = (h/q^2)(1/(M+N))$ is the ballistic resistance of the channel. See Appendix E for derivation. Combining Eq. (27) with Eq. (28) yields

$$\begin{aligned} & \frac{1}{|\langle v_x \rangle|} \frac{\partial}{\partial t} \begin{bmatrix} 0 & 0 & 0 & 1 \\ 0 & 0 & 1 & 0 \\ 0 & 1 & 0 & 0 \\ 1 & 0 & 0 & 0 \end{bmatrix} \begin{Bmatrix} I_c R_B \\ 2V_s \\ I_s R_B \\ 2V_c \end{Bmatrix} + \frac{\partial}{\partial x} \begin{Bmatrix} I_c R_B \\ 2V_s \\ I_s R_B \\ 2V_c \end{Bmatrix} \\ &= \begin{bmatrix} 0 & 0 & 0 & 0 \\ 0 & 0 & -\frac{1}{\lambda_0} & \frac{\alpha p_0}{\lambda_0} \\ \frac{\alpha}{\lambda_s'} & -\frac{1}{\lambda_s} & 0 & 0 \\ -\frac{1}{\lambda} & \frac{1}{\alpha \lambda'} & 0 & 0 \end{bmatrix} \begin{Bmatrix} I_c R_B \\ 2V_s \\ I_s R_B \\ 2V_c \end{Bmatrix} \\ &- 2L_M \frac{\partial I_c}{\partial x} \begin{Bmatrix} 0 \\ 0 \\ \alpha p_0 \\ 1 \end{Bmatrix} + \frac{1}{|\langle v_x \rangle|} \frac{2}{C_E} \frac{\partial Q}{\partial t} \begin{Bmatrix} 1 \\ \alpha p_0 \\ 0 \\ 0 \end{Bmatrix} + \begin{Bmatrix} R_B i^c \\ 2\Delta v^s \\ R_B i^s \\ 2\Delta v^s \end{Bmatrix}, \end{aligned} \quad (29)$$

with the external contact terms given by

$$\begin{aligned} i^c &= i_U^+ + i_D^- + i_U^- + i_D^+, \\ i^s &= \alpha (i_U^+ - i_D^- + i_U^- - i_D^+) \\ \Delta v^c &= \frac{R_B}{2} (i_U^+ - i_D^- - i_U^- + i_D^+), \text{ and} \\ \Delta v^s &= \frac{\alpha R_B}{2} (i_U^+ + i_D^- - i_U^- - i_D^+). \end{aligned} \quad (30)$$

where i^c and i^s represent charge and spin currents entering into the channel from the external contact, Δv^c and Δv^s represent the change in channel charge and spin voltages in the region under the external contact. These contact related terms will be discussed in detail in the next section. Note that $\partial Q/\partial t$ on the right hand side of Eq. (29) related to the charge currents according to the continuity equation as

$$\frac{\partial Q}{\partial t} + \frac{\partial I_c}{\partial x} = i^c. \quad (31)$$

Transmission Line Model Parameters: We combine Eq. (29) with Eq. (31) to get

$$\begin{aligned} &\begin{bmatrix} C_{eff} & 0 \\ 0 & C_Q \end{bmatrix} \frac{\partial}{\partial t} \begin{Bmatrix} V_c \\ V_s \end{Bmatrix} + \begin{bmatrix} 0 & 0 \\ 0 & G_{sh} \end{bmatrix} \begin{Bmatrix} V_c \\ V_s \end{Bmatrix} + \frac{\partial}{\partial x} \begin{Bmatrix} I_c \\ I_s \end{Bmatrix} \\ &+ \begin{bmatrix} 0 & 0 \\ p_0 g_m L_M & 0 \end{bmatrix} \frac{\partial}{\partial t} \begin{Bmatrix} I_c \\ I_s \end{Bmatrix} = \begin{bmatrix} 0 & 0 \\ p_0 \gamma_s & 0 \end{bmatrix} \begin{Bmatrix} I_c \\ I_s \end{Bmatrix} + \begin{Bmatrix} i^c \\ i^s \end{Bmatrix}, \end{aligned} \quad (32)$$

and

$$\begin{aligned} &\begin{bmatrix} L_{eff} & 0 \\ 0 & L_K \end{bmatrix} \frac{\partial}{\partial t} \begin{Bmatrix} I_c \\ I_s \end{Bmatrix} + \begin{bmatrix} R_c & 0 \\ 0 & R_s \end{bmatrix} \begin{Bmatrix} I_c \\ I_s \end{Bmatrix} + \frac{\partial}{\partial x} \begin{Bmatrix} V_c \\ V_s \end{Bmatrix} \\ &- \begin{bmatrix} 0 & 0 \\ p_0 r_m C_{eff} & 0 \end{bmatrix} \frac{\partial}{\partial t} \begin{Bmatrix} V_c \\ V_s \end{Bmatrix} = \begin{bmatrix} 0 & p_0 \eta_c \\ p_0 \eta_s & 0 \end{bmatrix} \begin{Bmatrix} V_c \\ V_s \end{Bmatrix} \\ &+ \begin{Bmatrix} \Delta v^c \\ \Delta v^s \end{Bmatrix}, \end{aligned} \quad (33)$$

with the following model parameters: $C_{eff} = \frac{C_Q C_E}{C_Q + C_E}$,

$$\begin{aligned} L_{eff} &= L_M + L_K, \quad C_Q = \frac{2}{R_B |\langle v_x \rangle|}, \quad L_K = \frac{R_B}{2 |\langle v_x \rangle|}, \quad R_c = \frac{R_B}{2\lambda}, \\ R_s &= \frac{R_B}{2\lambda_0}, \quad G_{sh} = \frac{2}{R_B \lambda_s}, \quad p_0 \eta_c = \frac{1}{\alpha \lambda'}, \quad \eta_s = \frac{\alpha}{\lambda_0}, \\ p_0 \gamma_s &= \frac{\alpha}{\lambda'_s}, \quad g_m = \frac{2\alpha}{R_B}, \quad r_m = \frac{\alpha R_B C_Q}{2 C_E}, \quad V_m = \eta_c V_s, \\ V_n &= \eta_s V_c + r_m I_{em}, \quad \text{and} \quad I_n = \gamma_s I_c - g_m V_{em}. \end{aligned} \quad \text{Eqs. (32)-(33) are same as Eqs. (2)-(3) with the external contact terms.}$$

Mean Free Paths: We have three distinct mean free paths in Eq. (29), given by

$$\begin{aligned} \frac{1}{\lambda} &= \left(\frac{r_{s2}}{N} + \frac{r_{s1}}{M} \right) + r \left(\frac{1}{N} + \frac{1}{M} \right), \\ \frac{1}{\lambda_0} &= (r + t_s) \left(\frac{1}{N} + \frac{1}{M} \right), \text{ and} \\ \frac{1}{\lambda_s} &= \left(\frac{r_{s2}}{N} + \frac{r_{s1}}{M} \right) + t_s \left(\frac{1}{N} + \frac{1}{M} \right), \end{aligned} \quad (34)$$

where λ , λ_0 , and λ_s determine the series charge resistance R_c , the series spin resistance R_s , and the shunt spin conductance G_{sh} respectively. G_{sh} takes into account the spin relaxation process. The other terms of Eq. (29) are given by

$$\begin{aligned} \frac{1}{\lambda'} &= \left(\frac{r_{s2}}{N} - \frac{r_{s1}}{M} \right) + r \left(\frac{1}{N} - \frac{1}{M} \right), \text{ and} \\ \frac{1}{\lambda'_s} &= \left(\frac{r_{s2}}{N} - \frac{r_{s1}}{M} \right) + t_s \left(\frac{1}{N} - \frac{1}{M} \right), \end{aligned} \quad (35)$$

representing spin-charge coupling involving scattering rates. Here, λ'_s and λ' cause a charge induced spin signal and spin induced charge signal respectively. λ'_s and λ' are non-zero for $r_{s1}/M \neq r_{s2}/N$ even if $M = N$ (i.e. normal metal), which indicate a purely scattering induced spin-charge coupling. To avoid this, we assume that the reflection with spin flip per mode per unit length is same in the channel (i.e. $r_{s1}/M = r_{s2}/N$), which leads to

$$\frac{1}{\lambda'_s} = t_s \left(\frac{1}{N} - \frac{1}{M} \right) = \frac{p_0}{\lambda_t} \quad \text{and} \quad \frac{1}{\lambda'} = r \left(\frac{1}{N} - \frac{1}{M} \right) = \frac{p_0}{\lambda_r}.$$

IV. MODEL WITH EXTERNAL CONTACT

In this section, we incorporate external contact into our transmission line model in Fig. 1. The currents from the external contact in Eq. (27) are given by [23]

$$\begin{aligned} i_U^+ &= \frac{q^2}{h} M g_u \left(v_u - \frac{\tilde{\mu}(U^+)}{q} \right), \\ i_D^+ &= \frac{q^2}{h} N g_d \left(v_d - \frac{\tilde{\mu}(D^+)}{q} \right), \\ i_U^- &= \frac{q^2}{h} N g_u \left(v_u - \frac{\tilde{\mu}(U^-)}{q} \right), \\ \text{and } i_D^- &= \frac{q^2}{h} M g_d \left(v_d - \frac{\tilde{\mu}(D^-)}{q} \right). \end{aligned} \quad (36)$$

Here, v_u and v_d are up and down spin voltages at the external contact respectively. g_u and g_d are up and down spin conductances per unit mode per unit length of the contact. The contact can be either NM ($g_u = g_d$) or FM ($g_u \neq g_d$). Combining Eqs. (30) and (36), the external contact terms are derived as

$$\begin{Bmatrix} i^c \\ i^s \end{Bmatrix} = G_0 \begin{bmatrix} 1 & p_f \\ \alpha p_f & 1 \end{bmatrix} \begin{Bmatrix} v_c - V_c \\ v_s - V_s \end{Bmatrix}, \text{ and} \quad (37)$$

$$\begin{Bmatrix} \Delta v^c \\ \Delta v^s \end{Bmatrix} = \frac{G_0 R_B}{2} \begin{bmatrix} p_f & 1 \\ \alpha & p_f \end{bmatrix} \begin{Bmatrix} p_0 v_c - \frac{I_s R_B}{2\alpha} \\ p_0 v_s - \frac{\alpha I R_B}{2} \end{Bmatrix}, \quad (38)$$

where $p_f = (g_u - g_d)/(g_u + g_d)$ is the contact polarization and $G_0 = (M + N)(g_u + g_d)$ is the contact conductance

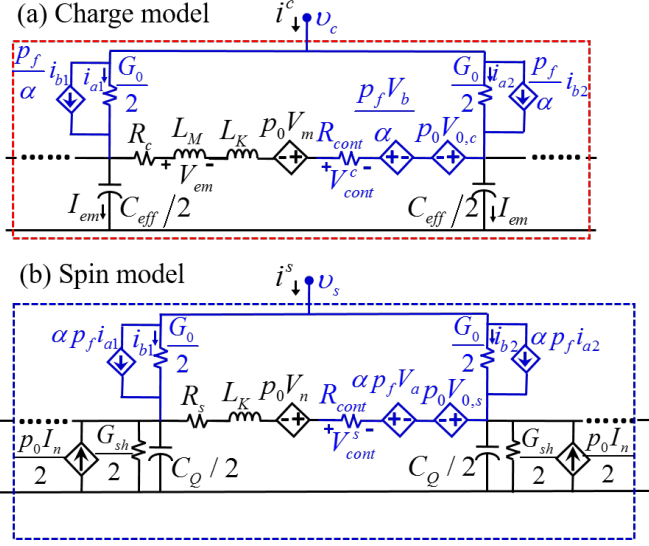


FIG. 3. Transmission line model for channels with spin-momentum locking (SML) with external contact. The (a) charge and (b) spin models are coupled through dependent sources proportional to the degree of SML (p_0). Components for external contacts are shown with blue color and correspond to Eqs. (37) and (38). Note that the model reduces to that shown in Fig. 1 in the limit $G_0 \rightarrow 0$.

per unit length. $p_f = 0$ corresponds to NM contact. The transmission line model with external contact is shown in Fig. 3 with external contact related components indicated with blue color. Note that the model in Fig. 3 reduces to that shown in Fig. 1 in the limit $G_0 \rightarrow 0$. The model can be incorporated in a circuit solver like SPICE and we can attach a number of such models (with or without contact) in a distributed manner using standard circuit rules to simulate a structure of interest.

Here, i^c and i^s in Eq. (37) are the charge and spin currents respectively entering the channel from the external contact. The diagonal terms are charge and spin conductances G_0 of the contact respectively. The off-diagonal terms are modeled with dependent current sources parallel to the charge and spin contact conductances, depending on the currents through the spin and charge contact conductances with gain factors p_f/α and αp_f respectively. The terms Δv^c and Δv^s in Eq. (38) represent additional change in the channel region under the contact, which have been modeled using additional series components with the parameters: $R_{cont} = \frac{G_0 R_B^2}{4}$, $V_{0,c} = \frac{G_0 R_B}{2} \left(\frac{v_s}{\alpha} + p_f v_c \right)$, and $V_{0,s} = \frac{G_0 R_B}{2} (\alpha v_c + p_f v_s)$. Note that these parameters are proportional to G_0 and negligible for potentiometric contacts where G_0 is low. Eq. (37) has been used in our earlier spin-circuit approach as FM|NM interface module (see for example, [45, 46], and references therein) and effects in Eq. (38) was ignored.

Presence of any contact (FM or NM) with conductance G_0 increases the effective channel resistance by R_{cont} for both charge and spin, irrespective of p_0 . This effect exists even if the channel is NM, which we have further evaluated in Appendix F using standard mesoscopic view [26] with two electrochemical potentials for forward and backward moving states. R_{cont} is negligible for low contact conductance and increases proportional to G_0 . This corresponds a reduction in channel current under a highly conductive contact. If the contact is FM (i.e. $p_f \neq 0$), there is an additional voltage change in charge and spin models (see Fig. 3), which are proportional to the voltage drop across R_{cont} in spin and charge models (V_{cont}^s and V_{cont}^c) respectively. In addition to the effects mentioned above, in a channel with SML there is an additional change in charge and spin voltages along \hat{x} -direction in the channel by $p_0 V_{0,c}$ and $p_0 V_{0,s}$ respectively.

Steady-State Model: At steady-state ($\partial/\partial t \rightarrow 0$), the transmission line model in (32) and (33) becomes

$$\begin{aligned} \frac{d}{dx} I_c &= i^c, \\ \frac{d}{dx} V_c &= -R_c I_c + p_0 \eta_c V_s + \Delta v^c, \\ \frac{d}{dx} I_s &= -G_{sh} V_s + p_0 \gamma_s I_c + i^s, \text{ and} \\ \frac{d}{dx} V_s &= -R_s I_s + p_0 \eta_s V_c + \Delta v^s. \end{aligned} \quad (39)$$

The steady-state form with two components: charge and z -polarization of spin is equivalent to our prior proposed time-independent semiclassical equations with four electrochemical potentials [23] and all our previous results can be reproduced from Eq. (39) as well. Note that under steady-state condition ($\partial/\partial t \rightarrow 0$), the capacitors and inductors in Fig. 3 becomes open and short respectively. For NM channels ($p_0 = 0$) without external contact ($G_0 \rightarrow 0$), Eq. (39) becomes standard diffusion equations for charge and spin, given by

$$\frac{d^2}{dx^2} V_c = 0, \text{ and } \frac{d^2}{dx^2} V_s = \frac{V_s}{\lambda_{sf}^2}, \quad (40)$$

where the spin diffusion length is given by $\lambda_{sf} = 1/\sqrt{R_s G_{sh}} = \sqrt{\lambda_0 \lambda_s}$.

V. SUMMARY

We have proposed a two component (charge and z -component of spin) transmission line model for channels with spin-momentum locking (SML) which can be applied to diverse classes of materials e.g. topological insulators, heavy metals, and narrow bandgap semiconductors. A steady-state version of the model has been previously used to make novel predictions on SML channels [23] some of which have already been observed experimentally. The model presented here is a new addition to

our experimentally benchmarked and SPICE compatible multi-physics framework [44–46], which will enable both time-dependent and steady-state analysis on SML channels. The model is derived from time-dependent Boltzmann transport equation with four electrochemical potentials for four groups of states (U^+ , D^+ , U^- , and D^-) depending on the sign of z -component of spin (up (U) or down (D)) and the sign of x -component of group velocity (+ or -). Such classification in steady-state, can be viewed as a combination of the Valet-Fert equation [25] with the mesoscopic view [26], widely used for normal metal channels. For a normal metal channel, the time-dependent model presented here decouples into (i) the well-known transmission line model for charge transport in quantum wires [47–49] and (ii) the time-dependent version of Valet-Fert equation [25]. Our model shows the expected spin-charge separation with two distinct velocities for charge and spin, which persist even in channels exhibiting SML. However, the lower velocity signal is purely spin while the higher velocity signal is largely charge with an additional spin component proportional to the degree of SML.

This work was supported by FAME, one of six centers of STARnet, a Semiconductor Research Corporation program sponsored by MARCO and DARPA.

Appendix A: Charge and spin velocity

This appendix provides the derivation of eigenvalues and eigenvectors of Eqs. (2) and (3) to find the charge and spin velocities and their coupling while propagation.

The matrix form of Eqs. (2) and (3) is given by

$$\begin{aligned} & \begin{bmatrix} C_{eff} & 0 & 0 & 0 \\ 0 & C_Q & p_0 g_m L_M & 0 \\ 0 & 0 & L_{eff} & 0 \\ -p_0 r_m C_{eff} & 0 & 0 & L_K \end{bmatrix} \frac{\partial}{\partial t} \begin{bmatrix} V_c \\ V_s \\ I_c \\ I_s \end{bmatrix} \\ & + \begin{bmatrix} 0 & 0 & 0 & 0 \\ 0 & G_{sh} & -p_0 \gamma_s & 0 \\ 0 & -p_0 \eta_c & R_c & 0 \\ -p_0 \eta_s & 0 & 0 & R_s \end{bmatrix} \begin{bmatrix} V_c \\ V_s \\ I_c \\ I_s \end{bmatrix} \\ & = - \begin{bmatrix} 0 & 0 & 1 & 0 \\ 0 & 0 & 0 & 1 \\ 1 & 0 & 0 & 0 \\ 0 & 1 & 0 & 0 \end{bmatrix} \frac{\partial}{\partial x} \begin{bmatrix} V_c \\ V_s \\ I_c \\ I_s \end{bmatrix}. \end{aligned} \quad (A1)$$

In order to find the velocities, we first ignore the lossy term linear with $\{V_c, V_s, I_c, I_s\}^T$ assuming low loss limit and then apply $\partial/\partial t \equiv -j\omega$ and $\partial/\partial x \equiv jk$ where ω and k are angular velocity and wave vector respectively. Noting that the signal velocity is given by $v_g \equiv \omega/k$ we

have

$$v_g \begin{bmatrix} V_c \\ V_s \\ I_c \\ I_s \end{bmatrix} = \begin{bmatrix} 0 & 0 & \frac{1}{C_{eff}} & 0 \\ -\frac{p_0 g_m L_M}{C_Q L_{eff}} & 0 & 0 & \frac{1}{C_Q} \\ \frac{1}{L_{eff}} & 0 & 0 & 0 \\ 0 & \frac{1}{L_K} & \frac{p_0 r_m}{L_K} & 0 \end{bmatrix} \begin{bmatrix} V_c \\ V_s \\ I_c \\ I_s \end{bmatrix}. \quad (A2)$$

and the eigenvalues give the velocities in Eqs. (4) and (6). For a particular eigenvalue v_g , we can write the following equation from Eq. (A2)

$$\begin{aligned} & \begin{bmatrix} -v_g & \frac{1}{C_{eff}} \\ \frac{1}{L_{eff}} & -v_g \end{bmatrix} \begin{bmatrix} V_c \\ I_c \end{bmatrix} = \begin{bmatrix} 0 \\ 0 \end{bmatrix}, \\ & \begin{bmatrix} -v_g & \frac{1}{C_Q} \\ \frac{1}{L_K} & -v_g \end{bmatrix} \begin{bmatrix} V_s \\ I_s \end{bmatrix} = p_0 \begin{bmatrix} \frac{g_m L_M}{C_Q L_{eff}} V_c \\ -\frac{r_m}{L_K} I_c \end{bmatrix}. \end{aligned} \quad (A3)$$

For the eigenvalue $v_g = v_{g,s} = 1/\sqrt{L_K C_Q}$ in Eq. (A3) we have $V_c = I_c = 0$ and assuming $I_s = 1$ we get Eq. (5). Again, for the eigenvalue $v_g = v_{g,c} = 1/\sqrt{L_{eff} C_{eff}}$ we get Eq. (7) assuming $I_c = 1$.

Appendix B: Derivation of semiclassical model

This appendix provides the derivation of Eq. (12), starting from the Boltzmann transport equation in Eq. (8).

We apply a variable transformation $\xi(x, t, \vec{p}, \vec{s}) \equiv E(x, t, \vec{p}, \vec{s}) - \mu(x, t, \vec{p}, \vec{s})$ on the left hand side of Eq. (8), which yields

$$\begin{aligned} \frac{\partial f}{\partial t} &= \frac{\partial f}{\partial \xi} \left(\frac{\partial E}{\partial t} - \frac{\partial \mu}{\partial t} \right), \\ v_x \frac{\partial f}{\partial x} &= v_x \frac{\partial f}{\partial \xi} \left(\frac{\partial E}{\partial x} - \frac{\partial \mu}{\partial x} \right), \text{ and} \\ F_x \frac{\partial f}{\partial p_x} &= F_x \frac{\partial f}{\partial \xi} \left(\frac{\partial E}{\partial p_x} - \frac{\partial \mu}{\partial p_x} \right). \end{aligned} \quad (B1)$$

We first substitute $F_x = -\frac{\partial E}{\partial x}$ and $v_x = \frac{\partial E}{\partial p_x}$. Finally, we set $\frac{\partial f}{\partial \xi} = \frac{\partial f_0}{\partial E}$ to get the left hand side of Eq. (12).

On the right hand side of Eq. (8), we expand both f and f' into Taylor series around $f_0 = 1/(1 + \exp((E(x, \vec{p}, s) - \mu_0)/k_B T))$ with constant electrochemical potential μ_0 . We set $\xi'(x, t, \vec{p}', s') \equiv E(x, t, \vec{p}', s') - \mu(x, t, \vec{p}', s')$ and $\xi_0(x, \vec{p}, s) \equiv E(x, \vec{p}, s) -$

μ_0 and assume that ξ and ξ' are close to ξ_0 which gives

$$\begin{aligned} f &\approx f_0 + \left(-\frac{\partial f}{\partial \xi}\right)_{\xi=\xi_0} (\xi - \xi_0), \text{ and} \\ f' &\approx f_0 + \left(-\frac{\partial f}{\partial \xi'}\right)_{\xi'=\xi_0} (\xi' - \xi_0). \end{aligned} \quad (\text{B2})$$

We set $\left(\frac{\partial f}{\partial \xi}\right)_{\xi=\xi_0} = \left(\frac{\partial f}{\partial \xi'}\right)_{\xi'=\xi_0} = \frac{\partial f_0}{\partial E}$. Thus the right hand side of Eq. (8) becomes

$$f - f' = \left(-\frac{\partial f_0}{\partial E}\right) (\xi - \xi') = \left(\frac{\partial f_0}{\partial E}\right) (\mu - \mu'), \quad (\text{B3})$$

noting that $E(x, t, \vec{p}', s') = E(x, t, \vec{p}, s)$ in the elastic scattering limit.

Appendix C: E - p relation

This appendix provides the derivation of Eq. (16), starting from the E - p relation in Eq. (14).

Differentiating Eq. (14) with respect to time t yields

$$\frac{\partial E}{\partial t} = \left(\frac{\vec{p} - q\vec{A}}{m} + s v_0 \frac{\vec{p} - q\vec{A}}{|\vec{p} - q\vec{A}|}\right) \cdot \left(-q \frac{\partial \vec{A}}{\partial t}\right) + \frac{\partial U_E}{\partial t}. \quad (\text{C1})$$

The velocity $\vec{v}(E) = \nabla_{\vec{p}} E$ is derived from Eq. (14) as

$$\vec{v}(E) = \frac{\vec{p} - q\vec{A}}{m} + s v_0 \frac{\vec{p} - q\vec{A}}{|\vec{p} - q\vec{A}|}. \quad (\text{C2})$$

Combining Eqs. (C1) and (C2) yields Eq. (15). Note that Eq. (C2) can be written as

$$\vec{v}(E) = \left(\frac{|\vec{p} - q\vec{A}|}{m} + s v_0\right) \frac{\vec{p} - q\vec{A}}{|\vec{p} - q\vec{A}|}. \quad (\text{C3})$$

where $\frac{\vec{p} - q\vec{A}}{|\vec{p} - q\vec{A}|}$ is a unit vector along $\vec{p} - q\vec{A}$. From Eq. (14) we get

$$|\vec{p} - q\vec{A}| = -s m v_0 \pm m \sqrt{v_0^2 + \frac{2(E - U_E)}{m}}, \quad (\text{C4})$$

noting that $s^2 = 1$. Thus from Eq. (C3) we get

$$\vec{v}(E) = \pm \sqrt{v_0^2 + \frac{2(E - U_E)}{m}} \frac{\vec{p} - q\vec{A}}{|\vec{p} - q\vec{A}|}. \quad (\text{C5})$$

Note that the magnitude of the velocity for a particular energy of interest is same for all four groups in Eq. (18) for the Rashba Hamiltonian in Eq. (13) considered here.

Appendix D: Scattering Rates

This appendix provides the derivation of the scattering matrix in Eq. (25).

The scattering rate related term on the right hand side of Eq. (24) is evaluated using the condition in Eq. (III) as

$$\begin{aligned} \tilde{S}(\mathfrak{R}) &= -\frac{\hbar}{L} \sum_{\vec{p}, s \in \mathfrak{R}} \sum_{\vec{p}', s'} S(\vec{p}, s \leftrightarrow \vec{p}', s') \left(-\frac{\partial f_0}{\partial E}\right) (\mu - \mu') \\ &= -\hat{S}_{\mathfrak{R} \leftrightarrow U^+} \langle \mu(\mathfrak{R}) \rangle - \hat{S}_{\mathfrak{R} \leftrightarrow D^-} \langle \mu(\mathfrak{R}) \rangle - \hat{S}_{\mathfrak{R} \leftrightarrow U^-} \langle \mu(\mathfrak{R}) \rangle \\ &\quad - \hat{S}_{\mathfrak{R} \leftrightarrow D^+} \langle \mu(\mathfrak{R}) \rangle + \hat{S}_{U^+ \leftrightarrow \mathfrak{R}} \langle \mu(U^+) \rangle + \hat{S}_{D^- \leftrightarrow \mathfrak{R}} \langle \mu(D^-) \rangle \\ &\quad + \hat{S}_{U^- \leftrightarrow \mathfrak{R}} \langle \mu(U^-) \rangle + \hat{S}_{D^+ \leftrightarrow \mathfrak{R}} \langle \mu(D^+) \rangle, \end{aligned} \quad (\text{D1})$$

$$\text{where } \hat{S}_{\mathfrak{R} \leftrightarrow \mathfrak{R}'} = \frac{\hbar}{L} \sum_{\vec{p}, s \in \mathfrak{R}} \sum_{\vec{p}', s' \in \mathfrak{R}'} S(\vec{p}, s' \leftrightarrow \vec{p}, s) \left(\frac{\partial f_0}{\partial E}\right).$$

For the group $\mathfrak{R} \equiv U^+, D^-, U^-,$ and D^+ , we have from Eq. (D1)

$$\begin{aligned} \tilde{S}(U^+) &= -\hat{S}_{U^+ \leftrightarrow D^-} \langle \mu(U^+) \rangle - \hat{S}_{U^+ \leftrightarrow U^-} \langle \mu(U^+) \rangle \\ &\quad - \hat{S}_{U^+ \leftrightarrow D^+} \langle \mu(U^+) \rangle + \hat{S}_{U^+ \leftrightarrow D^-} \langle \mu(D^-) \rangle \\ &\quad + \hat{S}_{U^+ \leftrightarrow U^-} \langle \mu(U^-) \rangle + \hat{S}_{U^+ \leftrightarrow D^+} \langle \mu(D^+) \rangle, \end{aligned} \quad (\text{D2})$$

$$\begin{aligned} \tilde{S}(D^-) &= -\hat{S}_{U^+ \leftrightarrow D^-} \langle \mu(D^-) \rangle - \hat{S}_{D^- \leftrightarrow U^-} \langle \mu(D^-) \rangle \\ &\quad - \hat{S}_{D^- \leftrightarrow D^+} \langle \mu(D^-) \rangle + \hat{S}_{U^+ \leftrightarrow D^-} \langle \mu(U^+) \rangle \\ &\quad + \hat{S}_{D^- \leftrightarrow U^-} \langle \mu(U^-) \rangle + \hat{S}_{D^- \leftrightarrow D^+} \langle \mu(D^+) \rangle, \end{aligned} \quad (\text{D3})$$

$$\begin{aligned} \tilde{S}(U^-) &= -\hat{S}_{U^+ \leftrightarrow U^-} \langle \mu(U^-) \rangle - \hat{S}_{D^- \leftrightarrow U^-} \langle \mu(U^-) \rangle \\ &\quad - \hat{S}_{U^- \leftrightarrow D^+} \langle \mu(U^-) \rangle + \hat{S}_{U^+ \leftrightarrow U^-} \langle \mu(U^+) \rangle \\ &\quad + \hat{S}_{D^- \leftrightarrow U^-} \langle \mu(D^-) \rangle + \hat{S}_{U^- \leftrightarrow D^+} \langle \mu(D^+) \rangle, \end{aligned} \quad (\text{D4})$$

and

$$\begin{aligned} \tilde{S}(D^+) &= -\hat{S}_{U^+ \leftrightarrow D^+} \langle \mu(D^+) \rangle - \hat{S}_{D^- \leftrightarrow D^+} \langle \mu(D^+) \rangle \\ &\quad - \hat{S}_{U^- \leftrightarrow D^+} \langle \mu(D^+) \rangle + \hat{S}_{U^+ \leftrightarrow D^+} \langle \mu(U^+) \rangle \\ &\quad + \hat{S}_{D^- \leftrightarrow D^+} \langle \mu(D^-) \rangle + \hat{S}_{U^- \leftrightarrow D^+} \langle \mu(U^-) \rangle. \end{aligned} \quad (\text{D5})$$

Eqs. (D2), (D3), (D4), and (D5) together yields the scattering matrix in Eq. (25).

Appendix E: Charge and Spin Currents and Voltages

This appendix provides the derivation of the Eq. (28).

The current in any group is given by

$$I(\mathfrak{R}) = \frac{q}{L} \sum_{\vec{p}, s \in \mathfrak{R}} v_x f(x, t, \vec{p}, s). \quad (\text{E1})$$

where f is given by Eq. (9). Under the linear response approximation, we can write

$$f(x, t, \vec{p}, s) \approx f_0 + \left(-\frac{\partial f_0}{\partial E} \right) (\mu(x, t, \vec{p}, s) - \mu_0) \quad (\text{E2})$$

where, f_0 is given by Eq. (10) with constant electrochemical potential μ_0 . Thus from Eq. (E1), we can write

$$I(\mathfrak{R}) = \frac{q}{L} \left(f_0 \sum_{\vec{p}, s \in \mathfrak{R}} v_x + \frac{D_0(\mathfrak{R})}{2} \left(\langle v_x \mu \rangle_{\vec{p}, s \in \mathfrak{R}} - \mu_0 \langle v_x \rangle \right) \right), \quad (\text{E3})$$

where $D_0(\mathfrak{R})$ is given by Eq. (21) and the averaging is defined by Eq. (19).

We assume the following

$$\langle v_x \mu \rangle_{\vec{p}, s \in \mathfrak{R}} \approx \langle v_x \rangle \langle \mu \rangle_{\vec{p}, s \in \mathfrak{R}},$$

which results in

$$I(\mathfrak{R}) = \text{sgn}(\langle v_x \rangle) \frac{q}{h} n_m(\mathfrak{R}) \left(\langle \mu \rangle_{\vec{p}, s \in \mathfrak{R}} - \mu_0 \right) + \text{sgn}(|v_x|) \frac{q}{L} f_0 \sum_{\vec{p}, s \in \mathfrak{R}} |v_x|, \quad (\text{E4})$$

where $n_m(\mathfrak{R})$ is given by Eq. (23).

Charge Current

The charge current in the channel is given by

$$I_c = I(U^+) + I(D^+) - I(U^-) - I(D^-), \quad (\text{E5})$$

which in conjunction to Eq. (E4) yields

$$I_c = \frac{q}{h} \left[\frac{h}{L} f_0 \sum_{\vec{p}, s \in U^+} |v_x| + M(\mu(U^+) - \mu_0) \right] + \frac{q}{h} \left[\frac{h}{L} f_0 \sum_{\vec{p}, s \in D^+} |v_x| + N(\mu(D^+) - \mu_0) \right] - \frac{q}{h} \left[\frac{h}{L} f_0 \sum_{\vec{p}, s \in U^-} |v_x| + N(\mu(U^-) - \mu_0) \right] - \frac{q}{h} \left[\frac{h}{L} f_0 \sum_{\vec{p}, s \in D^-} |v_x| + M(\mu(D^-) - \mu_0) \right], \quad (\text{E6})$$

where $n_m(U^+) = n_m(D^-) = M$ and $n_m(U^-) = n_m(D^+) = N$. Note that (U^+, D^-) and (U^-, D^+) are time-reversal symmetric pairs, hence

$$\sum_{\vec{p}, s \in U^+} |v_x| = \sum_{\vec{p}, s \in D^-} |v_x|, \text{ and} \quad (\text{E7}) \\ \sum_{\vec{p}, s \in U^-} |v_x| = \sum_{\vec{p}, s \in D^+} |v_x|,$$

Thus the expression for charge current is given by

$$I_c = \frac{q}{h} (M\tilde{\mu}(U^+) - N\tilde{\mu}(U^-) + N\tilde{\mu}(D^+) - M\tilde{\mu}(D^-)), \quad (\text{E8})$$

where we defined $\tilde{\mu} = \mu - \mu_0$.

Spin Current

The spin current in the channel is given by

$$\tilde{I}_s = \alpha (I(U^+) + I(U^-) - I(D^+) - I(D^-)), \quad (\text{E9})$$

where $\alpha = 2/\pi$ is an angular averaging factor to take into account the average $\hat{z} \cdot \vec{s}$ on a half Fermi circle (see Fig. 2(a)). Eq. (E9) in conjunction to Eq. (E4) yields

$$\tilde{I}_s = \alpha \frac{q}{h} \left[\frac{h}{L} f_0 \sum_{\vec{p}, s \in U^+} |v_x| + M(\mu(U^+) - \mu_0) \right] - \alpha \frac{q}{h} \left[\frac{h}{L} f_0 \sum_{\vec{p}, s \in U^-} |v_x| + N(\mu(U^-) - \mu_0) \right] - \alpha \frac{q}{h} \left[\frac{h}{L} f_0 \sum_{\vec{p}, s \in D^+} |v_x| + N(\mu(D^+) - \mu_0) \right] + \alpha \frac{q}{h} \left[\frac{h}{L} f_0 \sum_{\vec{p}, s \in D^-} |v_x| + M(\mu(D^-) - \mu_0) \right]. \quad (\text{E10})$$

Applying the condition in Eq. (E7), we have the expression for channel spin current as

$$\tilde{I}_s = \alpha \frac{q}{h} (M\tilde{\mu}(U^+) - N\tilde{\mu}(U^-) - N\tilde{\mu}(D^+) + M\tilde{\mu}(D^-)) + 2\alpha \frac{q}{L} f_0 \left(\sum_{\vec{p}, s \in U^+} |v_x| - \sum_{\vec{p}, s \in U^-} |v_x| \right) \quad (\text{E11})$$

Note first term is zero at equilibrium condition $\mu(U^+) = \mu(U^-) = \mu(D^+) = \mu(D^-) = \mu_0$. However, the second term is non-zero even at equilibrium since

$$\sum_{\vec{p}, s \in U^+} |v_x| \neq \sum_{\vec{p}, s \in U^-} |v_x|$$

and represent the equilibrium spin current in the channel. We subtract the equilibrium part from our definition of spin current given by

$$I_s = \alpha \frac{q}{h} (M\tilde{\mu}(U^+) - N\tilde{\mu}(U^-) - N\tilde{\mu}(D^+) + M\tilde{\mu}(D^-)). \quad (\text{E12})$$

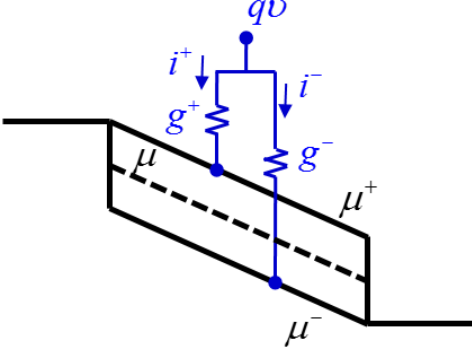


FIG. 4. Electrochemical potential profile in a normal metal channel and model for external contact.

Spin Voltage

The spin voltage in the channel is given by

$$qV_s = \alpha \frac{M\mu(U+) + N\mu(U-) - N\mu(D+) - M\mu(D-)}{2(M+N)}. \quad (\text{E13})$$

Subtracting each electrochemical potential by μ_0 which gives

$$qV_s = \alpha \frac{M\tilde{\mu}(U+) + N\tilde{\mu}(U-) - N\tilde{\mu}(D+) - M\tilde{\mu}(D-)}{2(M+N)}. \quad (\text{E14})$$

Charge Voltage

The charge voltage in the channel is given by

$$q\tilde{V}^c = \frac{M\mu(U+) + N\mu(U-) + N\mu(D+) + M\mu(D-)}{2(M+N)}. \quad (\text{E15})$$

Subtracting each electrochemical potential by μ_0 according to

$$qV^c = \frac{M\tilde{\mu}(U+) + N\tilde{\mu}(U-) + N\tilde{\mu}(D+) + M\tilde{\mu}(D-)}{2(M+N)}. \quad (\text{E16})$$

where $V_c = \tilde{V}_c - \frac{\mu_0}{q}$.

Eqs. (E8), (E12), (E14), and (E16) together can be written in a matrix form given by Eq. (28).

Appendix F: Effect of normal metal contact on normal metal channel

This appendix discusses the contact induced effective increase in the channel resistance using mesoscopic view with two electrochemical potentials for forward and backward moving states.

The diffusion equation for an arbitrary channel in terms of two electrochemical potentials for forward (μ^+) and backward (μ^-) moving states is given by [26]

$$\frac{d}{dx} \begin{Bmatrix} M\mu^+ \\ -M\mu^- \end{Bmatrix} = -\frac{M}{\lambda} \begin{bmatrix} 1 & -1 \\ -1 & 1 \end{bmatrix} \begin{Bmatrix} \mu^+ \\ \mu^- \end{Bmatrix} + \frac{h}{q} \begin{Bmatrix} i_c^+ \\ i_c^- \end{Bmatrix}, \quad (\text{F1})$$

where M is the total number of modes of the channel, λ is the mean free path. Here, i_c^+ and i_c^- are currents from an external normal metal contact, entering forward/backward moving states (see Fig. 4), given by

$$i_c^+ = g^+ M \left(v_c - \frac{\mu^+}{q} \right), \quad \text{and} \quad i_c^- = g^- M \left(v_c - \frac{\mu^-}{q} \right), \quad (\text{F2})$$

where v_c is the voltage at the external contact and g^+ and g^- are the external contact conductances connecting to forward and backward moving states of the channel.

The charge current in the channel is given by

$$I_c = \frac{q}{h} M (\mu^+ - \mu^-), \quad (\text{F3})$$

and charge potential in the channel is given by

$$\mu_c = \frac{\mu^+ + \mu^-}{2}. \quad (\text{F4})$$

Combining Eq. (F1) with Eqs. (F3) and (F4) yields

$$\frac{d}{dx} I_c = g_0 \left(v_c - \frac{\mu_c}{q} \right), \quad (\text{F5})$$

and

$$\frac{d}{dx} \left(-\frac{\mu_c}{q} \right) = \left(\frac{1}{\lambda G_B} + \frac{g_0}{4G_B^2} \right) I_c, \quad (\text{F6})$$

where g_0 is the contact conductance with $g_0/2 = Mg^+ = Mg^-$. The term on the right hand side of Eq. (F5) correspond to the current flowing into the channel from the external contact. The right hand side of Eq. (F6) shows that $g_0/4G_B^2$ effectively increases the channel resistance corresponding to less channel current under a highly conductive contact.

-
- [1] M. Z. Hasan and C. L. Kane, Rev. Mod. Phys. **82**, 3045 (2010).
 - [2] X.-L. Qi and S.-C. Zhang, Rev. Mod. Phys. **83**, 1057 (2011).
 - [3] Y. Fan and K. L. Wang, SPIN **06**, 1640001 (2016).
 - [4] I. M. Miron, K. Garello, G. Gaudin, P.-J. Zermatten, M. V. Costache, S. Auffret, S. Bandiera, B. Rodmacq, A. Schuhl, and P. Gambardella, Nature **476**, 189 (2011).
 - [5] T. Suzuki, S. Fukami, N. Ishiwata, M. Yamanouchi, S. Ikeda, N. Kasai, and H. Ohno, Appl. Phys. Lett. **98**, 142505 (2011).

- [6] C.-F. Pai, L. Liu, Y. Li, H. W. Tseng, D. C. Ralph, and R. A. Buhrman, *Appl. Phys. Lett.* **101**, 122404 (2012).
- [7] L. Liu, C.-F. Pai, Y. Li, H. W. Tseng, D. C. Ralph, and R. A. Buhrman, *Science* **336**, 555 (2012).
- [8] B. Yan, B. Stadtmüller, N. Haag, S. Jakobs, J. Seidel, D. Jungkenn, S. Mathias, M. Cinchetti, M. Aeschlimann, and C. Felser, *Nat. Commun.* **6**, 10167 (2015).
- [9] J. C. R. Sánchez, L. Vila, G. Desfonds, S. Gambarelli, J. P. Attané, J. M. De Teresa, C. Magén, and A. Fert, *Nat. Commun.* **4**, 2944 (2016).
- [10] P. R. Hammar and M. Johnson, *Phys. Rev. B* **61**, 7207 (2000).
- [11] Y. H. Park, H. Cheol Jang, H. C. Koo, H.-j. Kim, J. Chang, S. H. Han, and H.-J. Choi, *Journal of Applied Physics* **111**, 07 (2012).
- [12] R. H. Silsbee, *Journal of Physics: Condensed Matter* **16**, R179 (2004).
- [13] S. Tölle, U. Eckern, and C. Gorini, *Phys. Rev. B* **95**, 115404 (2017).
- [14] X. Liu and J. Sinova, *Phys. Rev. B* **86**, 174301 (2012).
- [15] X. Liu and J. Sinova, *Phys. Rev. Lett.* **111**, 166801 (2013).
- [16] E. G. Mishchenko, A. V. Shytov, and B. I. Halperin, *Phys. Rev. Lett.* **93**, 226602 (2004).
- [17] A. A. Burkov, A. S. Núñez, and A. H. MacDonald, *Phys. Rev. B* **70**, 155308 (2004).
- [18] A. A. Burkov and D. G. Hawthorn, *Phys. Rev. Lett.* **105**, 066802 (2010).
- [19] A. N. M. Zainuddin, S. Hong, L. Siddiqui, S. Srinivasan, and S. Datta, *Phys. Rev. B* **84**, 165306 (2011).
- [20] S. Hong, V. Diep, S. Datta, and Y. P. Chen, *Phys. Rev. B* **86**, 085131 (2012).
- [21] Y. Tserkovnyak and S. A. Bender, *Phys. Rev. B* **90**, 014428 (2014).
- [22] Y.-T. Chen, S. Takahashi, H. Nakayama, M. Althammer, S. T. B. Goennenwein, E. Saitoh, and G. E. W. Bauer, *Phys. Rev. B* **87**, 144411 (2013).
- [23] S. Sayed, S. Hong, and S. Datta, *Sci. Rep.* **6**, 35658 (2016).
- [24] S. Hong, S. Sayed, and S. Datta, *Sci. Rep.* **6**, 20325 (2016).
- [25] T. Valet and A. Fert, *Phys. Rev. B* **48**, 7099 (1993).
- [26] S. Datta, *Electronic Transport in Mesoscopic Systems* (Cambridge University Press, Cambridge, 1997).
- [27] C. H. Li, O. M. van 't Erve, J. T. Robinson, Y. Liu, L. Li, and J. B. T., *Nature Nanotechnol.* **9**, 20325 (2014).
- [28] J. Tang, L.-T. Chang, X. Kou, K. Murata, E. S. Choi, M. Lang, Y. Fan, Y. Jiang, M. Montazeri, W. Jiang, Y. Wang, L. He, and K. L. Wang, *Nano Letters* **14**, 5423 (2014).
- [29] A. Dankert, J. Geurs, M. V. Kamalakar, S. Charpentier, and S. P. Dash, *Nano Letters* **15**, 7976 (2015).
- [30] L. Liu, A. Richardella, I. Garate, Y. Zhu, N. Samarth, and C.-T. Chen, *Phys. Rev. B* **91**, 235437 (2015).
- [31] J. Tian, I. Miotkowski, S. Hong, and Y. P. Chen, *Sci. Rep.* **5**, 14293 (2015).
- [32] J. S. Lee, A. Richardella, D. R. Hickey, K. A. Mkhoyan, and N. Samarth, *Phys. Rev. B* **92**, 155312 (2015).
- [33] F. Yang, S. Ghatak, A. A. Taskin, K. Segawa, Y. Ando, M. Shiraishi, Y. Kanai, K. Matsumoto, A. Rosch, and Y. Ando, *Phys. Rev. B* **94**, 075304 (2016).
- [34] V. T. Pham, L. Vila, G. Zahnd, A. Marty, W. Saverio-Torres, M. Jamet, and J.-P. Attan, *Nano Lett.* **16**, 6755 (2016).
- [35] V. T. Pham, G. Zahnd, A. Marty, W. Saverio Torres, M. Jamet, P. Nol, L. Vila, and J. P. Attan, *Appl. Phys. Lett.* **109**, 192401 (2016).
- [36] P. Li and I. Appelbaum, *Phys. Rev. B* **93**, 220404 (2016).
- [37] P. M. Haney, H.-W. Lee, K.-J. Lee, A. Manchon, and M. D. Stiles, *Phys. Rev. B* **87**, 174411 (2013).
- [38] J. Sinova, S. O. Valenzuela, J. Wunderlich, C. H. Back, and T. Jungwirth, *Rev. Mod. Phys.* **87**, 1213 (2015).
- [39] A. Hoffmann, *IEEE Transactions on Magnetism* **49**, 5172 (2013).
- [40] H. L. Wang, C. H. Du, Y. Pu, R. Adur, P. C. Hammel, and F. Y. Yang, *Phys. Rev. Lett.* **112**, 197201 (2014).
- [41] H. J. Zhang, S. Yamamoto, Y. Fukaya, M. Maekawa, H. Li, A. Kawasuso, T. Seki, E. Saitoh, and K. Takanashi, *Sci. Rep.* **4**, 4844 (2014).
- [42] M. Hoesch, M. Muntwiler, V. N. Petrov, M. Hengsberger, L. Patthey, M. Shi, M. Falub, T. Greber, and J. Osterwalder, *Phys. Rev. B* **69**, 241401 (2004).
- [43] A. Tamai, W. Meevasana, P. D. C. King, C. W. Nicholson, A. de la Torre, E. Rozbicki, and F. Baumberger, *Phys. Rev. B* **87**, 075113 (2013).
- [44] K. Y. Camsari, S. Ganguly, S. Sayed, and S. Datta, "Modular approach to spintronics," (2013), <https://nanohub.org/groups/spintronics>.
- [45] K. Y. Camsari, S. Ganguly, and S. Datta, *Sci. Rep.* **5**, 10571 (2015).
- [46] S. Sayed, V. Q. Diep, K. Y. Camsari, and S. Datta, *Sci. Rep.* **6**, 28868 (2016).
- [47] P. J. Burke, *IEEE Transactions on Nanotechnology* **1**, 129 (2002).
- [48] P. J. Burke, *IEEE Transactions on Nanotechnology* **2**, 55 (2003).
- [49] S. Salahuddin, M. Lundstrom, and S. Datta, *IEEE Transactions on Electron Devices* **52**, 1734 (2005).
- [50] B. I. Halperin, *Journal of Applied Physics* **101**, 081601 (2007).
- [51] M. Polini and G. Vignale, *Phys. Rev. Lett.* **98**, 266403 (2007).
- [52] A. Schroer, B. Braunecker, A. Levy Yeyati, and P. Recher, *Phys. Rev. Lett.* **113**, 266401 (2014).
- [53] A. De Martino, R. Egger, K. Hallberg, and C. A. Balsero, *Phys. Rev. Lett.* **88**, 206402 (2002).
- [54] A. Calzona, M. Carrega, G. Dolcetto, and M. Sassetti, *Phys. Rev. B* **92**, 195414 (2015).
- [55] T. Stauber, G. Gómez-Santos, and L. Brey, *Phys. Rev. B* **88**, 205427 (2013).
- [56] A. V. Moroz, K. V. Samokhin, and C. H. W. Barnes, *Phys. Rev. Lett.* **84**, 4164 (2000).
- [57] S. Datta, *Lessons from Nanoelectronics: A New Perspective on Transport* (World Scientific Publishing Co. Pte. Ltd., Singapore, 2012).